

Ozonolysis and photolysis of alkene-terminated self-assembled monolayers on quartz nanoparticles: implications for photochemical aging of organic aerosol particles

Jiho Park, Anthony L. Gomez, Maggie L. Walser, Ao Lin and Sergey A. Nizkorodov*

Received 22nd February 2006, Accepted 11th April 2006

First published as an Advance Article on the web 25th April 2006

DOI: 10.1039/b602704k

Photolysis of alkene-terminated self assembled monolayers (SAM) deposited on Degussa SiO₂ nanoparticles is studied following oxidation of SAM with a gaseous ozone/oxygen mixture. Infrared cavity ring-down spectroscopy is used to observe gas-phase products generated during ozonolysis and subsequent photolysis of SAM in real time. Reactions taking place during ozonolysis transform alkene-terminated SAM into a photochemically active state capable of photolysis in the tropospheric actinic window ($\lambda > 295$ nm). Formaldehyde and formic acid are the observed photolysis products. Photodissociation action spectra of oxidized SAM and the observed pattern of gas-phase products are consistent with the well-established Criegee mechanism of ozonolysis of terminal alkenes. There is strong evidence for the presence of secondary ozonides (1,3,4-trioxalones) and other peroxides on the oxidized SAM surface. The data imply that photolysis plays a role in atmospheric aging of primary and secondary organic aerosol particles.

Introduction

Atmospheric aerosol particles play an important role in controlling global climate and air quality.^{1,2} Although there have been numerous studies of the impact of aerosol particles on climate, unresolved issues and discrepancies persist.³ Chemical aging of aerosol particles has recently attracted strong interest from atmospheric chemists⁴ because chemical properties of the air–particle interface may affect the ability of aerosol particles to act as cloud condensation nuclei (CCN).⁵ Field observations of aerosol composition show that a substantial fraction of tropospheric aerosol particles can be classified as organic.⁶ Surface organics are continuously oxidized by reactions with atmospheric oxidizers including ozone and hydroxyl radicals.⁷ Such heterogeneous oxidation reactions may lead to the modification of surface chemical composition and morphology of particles, resulting in a change in their CCN activities.

Ozone is the second most important oxidizer of biogenic atmospheric organics after the hydroxyl radical. It is especially effective in oxidation of molecules containing unsaturated carbon–carbon bonds.⁸ The generally accepted mechanism of ozonolysis of olefins^{9,10} includes a rate-limiting formation of a primary ozonide (POZ), followed by a rapid unimolecular decomposition of the POZ into a stable carbonyl and an unstable carbonyl oxide, followed by secondary reactions of the carbonyl oxide. The secondary reactions result in products with a variety of chemical properties, depending on the reac-

tion pathways. In an inert liquid environment, the carbonyl oxide normally reacts with the geminate carbonyl to form a secondary ozonide (SOZ). In the presence of water or other participating solvents, carbonyl oxides form organic peroxides. In the gas phase, the fates of energy-rich carbonyl oxides are usually dominated by various decomposition and isomerization processes.¹¹

In addition to altering the chemical composition, oxidation of organic aerosol particles is likely to affect their photochemical properties. The absorption spectrum of alkenes that were partly oxidized by ozone is expected to undergo a considerable shift to the red compared to that of parent alkene molecules. The increase in the absorption cross section is primarily due to aldehydes and peroxides formed during oxidation. Indeed, the maxima of gas phase absorption cross sections of aldehydes (~ 300 nm) and peroxides (< 280 nm) appear at longer wavelengths compared to those of alkenes (< 220 nm). If the absorption cross sections are significantly shifted into the tropospheric relevant window ($\lambda > 295$ nm) direct photolysis processes can become a factor in aging of organic aerosol particles. Such “photoaging” can act as an additional source of small organic molecules and free radicals in the atmosphere, and uniquely modify the surface properties of organic aerosol particles.

In the present work, alkene-terminated molecules adsorbed on the surface of silicon oxide are used as a surrogate for aerosol particles coated by an organic surfactant. The main objective of this work is to investigate the effect of oxidation by ozone on the photochemical properties of the organic surface. To this end, the UV photodissociation spectrum of the oxidized surface is measured using action spectroscopy,

Department of Chemistry, University of California, Irvine, CA 92697-2025, U.S.A. E-mail: nizkorod@uci.edu; Fax: +1-949-824-8571; Tel: +1-949-824-1262

wherein gas-phase formaldehyde and formic acid photolysis product concentrations are carefully measured at different excitation wavelengths.

Experiment

Powdery silicon oxide was functionalized to prepare SAM of alkene-terminated organic silanes using the method reported by Usher *et al.*¹² Briefly, SiO₂ powder (Degussa OX50) was dried at ~400 K overnight prior to use and dispersed in dry toluene (1.5 g per 100 ml). Ten drops (~210 mg) of 5-hexenyldimethylchlorosilane (Gelest) and five drops (~120 mg) of pyridine were added to the SiO₂/toluene suspension. The temperature of the resulting solution was kept at 360 K for about 3 h with vigorous stirring. Treated SiO₂ particles coated with 5-hexenyldimethylchlorosilane were collected using vacuum filtration and stored in dry toluene after washing them with clean toluene at least three times.

A fraction of the toluene slurry containing freshly prepared organic-coated SiO₂ powder (C₆ = SAM on SiO₂ nanoparticles) was transferred onto the inner wall of a quartz tube and dried by flowing nitrogen gas over it. Only one side of the tube was coated to allow UV radiation to enter the tube through the uncoated side. After installing the quartz tube between two highly reflective mirrors of a cavity ring-down spectrometer (Fig. 1), residual toluene was pumped out overnight before proceeding with the ozonolysis experiment.

All experiments were performed at room temperature (295 K). The SAM adsorbed on the inner wall of quartz tube (ID = 1.27 cm) was exposed to ozone in the dark at a concentration of ~10¹⁴–10¹⁵ molecules cm⁻³ until nearly complete oxidation of surface alkenes was achieved. The ozone concentration was considerably higher than a typical atmospheric value. However, this study mainly focused on the photolysis of ozonized terminal alkenes adsorbed on the silicone oxide surface, and not on the ozonolysis reaction. The carrier gas contained O₂ and He at a total pressure of 5–30 Torr. The gas-phase products of the ozonolysis of SAM were probed in real-time

using infrared cavity ring-down spectroscopy (IR-CRDS). In the majority of experiments, the film was oxidized on a time scale of 30–60 min making it possible to complete several IR-CRDS scans (5–10 min each) in the process. The IR-CRDS cavity was equipped with 99.98% reflective mirrors (diameter = 2 cm) optimized for the range around 3.3 μm (Los Gatos Research). The cavity mirrors were spaced by about 60 cm and protected by a constant purging flow of dry helium, resulting in empty cavity ring-down times on the order of 5–10 μs. A commercial pulsed optical parametric oscillator laser (Laser-Vision) with 0.1 cm⁻¹ spectral resolution, pumped by an Nd:YAG laser (Continuum), was used to optically pump the cavity. The region between 2910 and 2930 cm⁻¹, which contains easily identifiable lines of formaldehyde and formic acid, was used to quantitatively detect these two products. More details about the IR-CRDS system are provided in ref. 13.

Before the photolysis experiments, the cell containing ozonized SAM was evacuated in the dark for several hours to remove volatile products formed during ozonolysis. Radiation from a 150 W Xe-arc lamp was directed through a 295 nm long-pass filter or a monochromator to select the wavelength (resulting wavelength resolution ~10 nm), and the sample cell was illuminated at a right angle to the IR-CRDS cavity axis. The maximal UV-radiation power (at 310 nm) was 17.5 mW distributed over an irradiation area of 1 cm². The power was considerably lower for shorter irradiation wavelengths. The rest of the cell was protected from scattered radiation by foil. There was no correlation between the observed rate of photolysis and the location of the photolysis spot suggesting that the oxidized SAM was relatively homogeneous. All photolysis experiments were also carried out at room temperature (295 K) under slow flow conditions (~1–5 min cavity flushing time) using ultra high purity helium as a bath gas at 5–30 Torr. An optoacoustic reference spectrum of HCOOH vapor (1 Torr of HCOOH in 10–100 Torr N₂ buffer) was recorded in parallel with the IR-CRDS spectrum for wavelength calibration purposes.

Results

(a) Ozonolysis

Sample IR-CRDS absorption scans of gas phase products from ozonolysis (a) and subsequent photolysis (b) of SAM are shown in Fig. 2. The reference absorption spectrum of formaldehyde (c) and optoacoustic spectrum of formic acid (d) are also plotted for comparison. This lab previously reported¹⁴ that no HCHO or HCOOH gas-phase products are emitted during the ozonolysis of alkane SAM deposited on flat Si(111) wafers (ozone reacts very slowly with saturated hydrocarbons and it does not destroy the O–Si–C bridges in SAM). On the contrary, ozonolysis of alkene-terminated SAM on Si wafers generated HCHO as the major gas-phase product.¹⁴ The results obtained here are qualitatively similar but the signal-to-noise ratio is considerably improved because of the considerably larger combined surface area of SiO₂ nanoparticles compared to the Si wafer.

Similar to the results for Si wafers,¹⁴ large signals from HCHO and smaller signals from HCOOH were detected

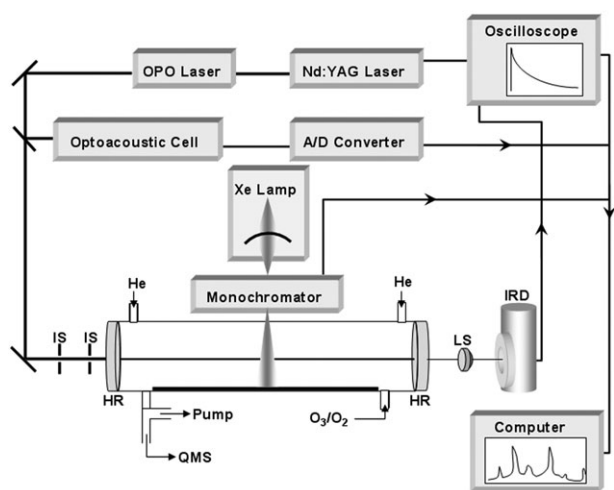


Fig. 1 Schematic diagram of the IR-CRDS setup. HR = highly reflective mirror; LS = focusing lens; IS = iris; IRD = IR Detector; QMS = quadrupole mass spectrometer.

during ozonolysis of alkene-terminated SAM on SiO₂ particles (Fig. 2(a)). The absolute ratio between HCHO and HCOOH formation was obtained by simulating the IR-CRDS spectra using the known absorption cross sections for these two molecules.¹⁵ The laser bandwidth (0.1 cm⁻¹) is larger than the bandwidth of individual ro-vibrational transitions in HCHO and HCOOH (0.01 cm⁻¹), which makes the apparent IR-CRDS absorption coefficient depend on concentration in a nonlinear way.¹³ However, the branching ratio obtained from well-isolated HCHO and HCOOH lines with comparable line strengths and intrinsic line widths is expected to be fairly quantitative.

Analysis of the IR-CRDS spectra provides an approximate ratio of HCOOH/HCHO = 0.65 ± 0.20. This ratio represents a time-averaged value over the initial stages of ozonolysis (~10 min). This time is comparable to the half-time for complete film oxidation and gas-SAM equilibration (~10 min). Our data suggest that the HCOOH/HCHO ratio remains approximately the same at later stages of ozonolysis implying that there is no drastic change in the mechanism of POZ decomposition as the organic film ages.

(b) Photolysis

A sample CRDS spectrum obtained during the broadband photolysis of the oxidized surface with a 295 nm long-pass filter is shown in Fig. 2(b). The spectrum unambiguously shows that both formaldehyde and formic acid are produced during photolysis. These molecules were not detected during

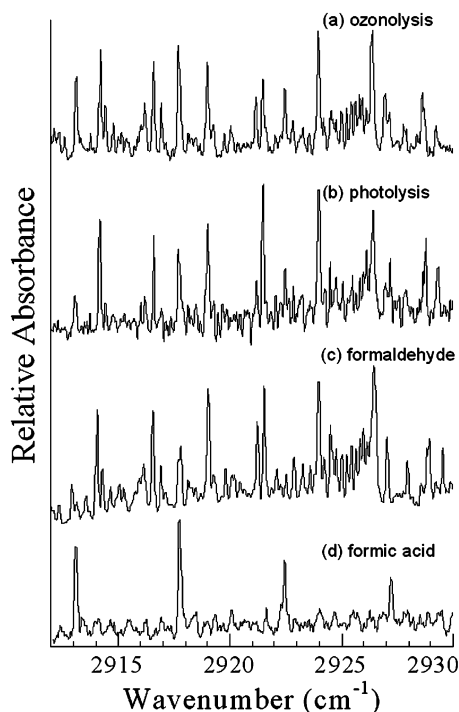


Fig. 2 IR-CRDS spectra of gas products from (a) ozonolysis and (b) photolysis ($\lambda > 295$ nm) of SAM on SiO₂ nanoparticles. Spectrum (b) was obtained after SAM was oxidized by ozone. Reference spectrum of formaldehyde (c) and optoacoustic spectrum of formic acid (d) are plotted for comparison.

UV irradiation of the SAM surface before it was processed with ozone. We also explicitly verified that the observed emission of HCHO and HCOOH was not a result of simple thermal desorption caused by radiative heating of the sample. A K-type thermocouple was attached to the sample cell during photolysis, and no significant temperature elevation at the irradiated surface was observed.

The primary focus of this work is the effect of oxidation of SAM on its photochemical activity in the tropospheric actinic window ($\lambda > 295$ nm). We studied the wavelength-dependent photolysis of the oxidized sample by taking its action photodissociation spectrum in the HCOOH product channel. Specifically, a small section (~1 cm²) of oxidized SAM was photolyzed with a tunable UV source, while keeping the IR-CRDS laser frequency fixed on a strong absorption line of formic acid at ~2917.9 cm⁻¹. Fig. 3 shows the observed change in formic acid concentration as a function of photolysis time at several different photolysis wavelengths. The steady-state is achieved after 10–20 min of photolysis, with the formic acid concentration at steady-state increasing at shorter photolysis wavelengths. We attribute the long time required to reach the steady-state to slow desorption of formic acid from high surface area SiO₂ particles.

The wavelength-dependent relative yield of formic acid corrected for the UV lamp power and quartz cell transmission is plotted in Fig. 4. The action spectrum is characteristic of absorption by peroxy groups, with the photodissociation yield of HCOOH smoothly increasing towards the blue end of the spectrum. It should be noted that significant formation of formic acid is detected at wavelengths where the initial alkene-terminated SAM is stable to photolysis. This observation is in

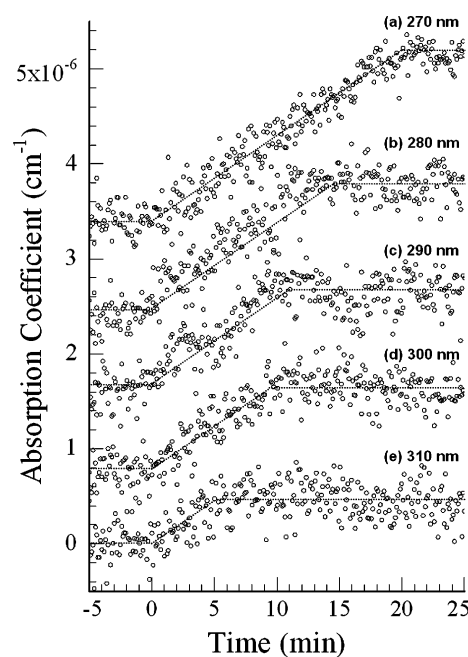


Fig. 3 Formic acid formation during photolysis of ozonized SAM as a function of photolysis time. Photolysis wavelengths are (a) 270 nm, (b) 280 nm, (c) 290 nm, (d) 300 nm, and (e) 310 nm. The baselines are offset, and dotted trace lines are added for clarity.

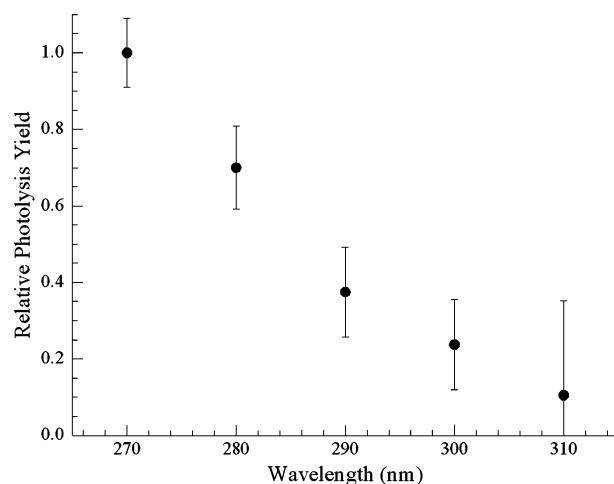


Fig. 4 Relative yield of formic acid from the photolysis of ozonized SAM as a function of the photolysis wavelength (normalized to the UV power).

line with the results from our study of photolysis of ozonized undecylenic acid with the same approach.¹³

We have attempted to characterize the surface products of SAM oxidation and photolysis by electrospray ionization mass spectrometry (ESI-MS). The ESI-MS approach was very helpful in unravelling the mechanism of ozonolysis and photolysis of undecylenic acid reported in ref. 13. Unfortunately, ESI-MS of products of SAM hydrolysis gave incomprehensibly complex mass spectra in both positive and negative ion mode. The authors of ref. 26 had similar difficulties in analyzing the composition of surface products of ozonolysis of SAM on Si wafers.

Discussion

(a) Ozonolysis

The general mechanism of ozonolysis of unsaturated hydrocarbons has been extensively studied by many research groups.^{14,16,17} The effect of light radiation during/after ozonolysis has not been significantly considered and it will be discussed in the latter parts of this paper. Only a brief discussion necessary to support the photolysis results is given in this section.

A schematic diagram of the primary reactions between alkene-terminated SAM and ozone is shown in Fig. 5. The POZ produced in the initial ozone-double bond addition decomposes in one of two ways to produce either formaldehyde and a surface-bound Criegee intermediate (I) or a surface-bound aldehyde (II) and a gas-phase Criegee intermediate (III). Product molecules that are not bound to the surface may then escape from the SAM environment into the gas-phase or undergo secondary reactions within the SAM.

Gas-phase ozonolysis of terminal alkenes is known to produce HCHO, HCOOH, and other volatile products. For example, a study by Neeb *et al.*¹⁸ showed that the branching ratio for the HCHO formation channel in ozonolysis of terminal alkenes at 730 Torr is 0.5, whereas the branching

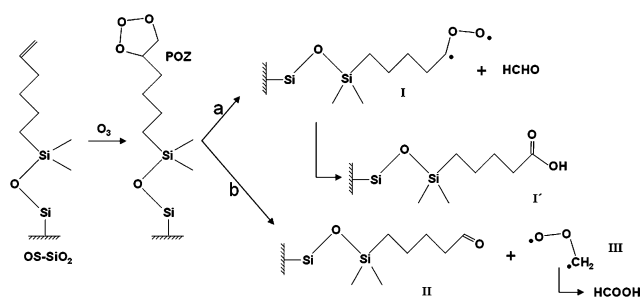


Fig. 5 Primary reactions taking place during ozonolysis of alkene-terminated SAM. OS-SiO₂ stands for the organic silane initially deposited on the SiO₂ surface.

ratio for the HCOOH formation channel through the isomerization of the Criegee intermediate is as low as 0.05. Ozonolysis of alkene-terminated SAM also favors the HCHO product.^{12,14}

Whereas the gas-phase products of ozonolysis of C₆ = SAM on SiO₂ nanoparticles are the same as previously observed, the HCOOH yield measured by the CRDS technique (0.4 ± 0.1) is substantially higher than that measured by mass-spectrometry study (<0.05).¹⁶ We stress that both methods of detection are prone to experimental artifacts: selective wall adsorption in mass-spectrometry and insufficient spectral resolution leading to non-linearity in absorbance in IR-CRDS. In addition, line strengths and pressure broadening coefficients for HCOOH transitions are not known precisely. However, it is possible that reduced stabilization of the escaping Criegee intermediate (III) under the low pressure conditions of this work does produce an increased yield of formic acid.

In view of the lack of strong spatial constraints in the decomposition of singly-substituted POZ, the branching ratio between channels a and b in Fig. 5 should be close to 1:1. The observed <50% yield of HCOOH implies that only a fraction of Criegee intermediate (III) can isomerize to HCOOH. One possibility is that III is rapidly decomposing into HCO, OH, CO₂, CO, H₂, and H₂O. The latter occurs, for example, in the gas phase ozone-propene reaction where yields of (CO + CO₂) were measured as 67% compared to 11% for formic acid.¹⁹ Our CRDS instrument in its present configuration is blind to CO and CO₂.

A more likely fate for III is stabilization followed by secondary reactions with neighboring SAM molecules. Indeed, there are several possible secondary reactions that take place in SAM after POZ decomposition. Criegee intermediates, I and III, can recombine with formaldehyde and surface aldehyde, respectively, to form surface secondary ozonides (sSOZ). This reaction is believed to be very efficient in liquids due to the solvent cage effect,²⁰ and it is conceivable that it also occurs in the semi-liquid SAM environment. The production of gas phase secondary ozonide (gSOZ) from the reaction between formaldehyde and Criegee intermediate (III) is also possible, and there have been several reports of gas phase SOZ formation from ozonation of alkenes in various pressure ranges.^{21–23}

As the SAM oxidation proceeds and surface products accumulate, new reaction channels open up due to the close

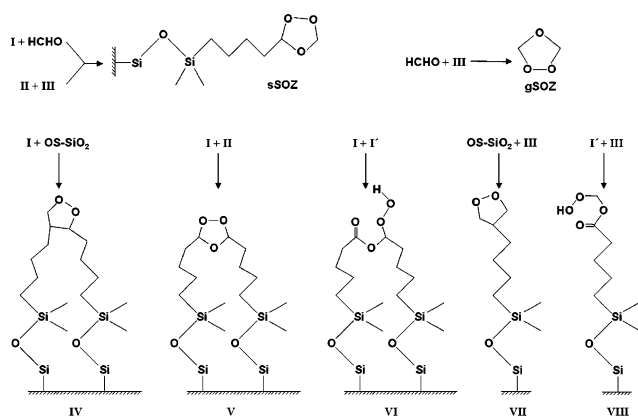


Fig. 6 Possible secondary reactions taking place during ozonolysis of alkene-terminated SAM.

proximity of surface bound molecules in SAM. For example, the association reaction of surface aldehyde (II) with surface Criegee intermediate (I) can form surface SOZ dimer (V) shown in Fig. 6. Criegee radical (I) can also attack double bonds and carboxylic groups in neighboring molecules to form other surface peroxides. Similar selective condensation reactions among the four species, I, I', III, and unreacted terminal alkene (OS-SiO₂) are also possible, again yielding various peroxides (structures IV, VI, VII, and VIII in Fig. 6). Even more complicated surface polymerization reactions initiated by the Criegee intermediates are possible as suggested in recent reports by Dreyfus *et al.*²⁴ and Hung *et al.*²⁵ For example, McIntire and co-workers²⁶ studied ozonolysis of unsaturated SAM on silica wafers using atomic force microscopy, and found unusually large organic aggregates with unknown chemical composition formed on the oxidized surface.

(b) Photolysis

Photolysis experiments lend strong support to the assumption that sSOZ and/or other peroxide products are present on the surface after ozonolysis. As described in the previous section, we found significant amounts of formic acid and formaldehyde produced during photolysis of oxidized SAM. Photolytic elimination of HCHO and HCOOH is not very common, and it strongly restricts the molecular nature of their possible photochemical precursors. For example, direct photochemical formation of HCHO and HCOOH from the photolysis of surface acid (I') and surface aldehyde (II) cannot occur at these excitation frequencies. Excitation of surface peroxides (IV–VIII) would sever the O–O bond but the resulting rearrangement products would remain attached to the surface and/or produce hydroxyl radicals. Although photolysis of gSOZ could give rise to both HCHO and HCOOH, gSOZ should be removed by pumping on the flow cell for several hours before starting the photolysis experiments. In addition, SOZ of ethene may not be stable enough to remain in the system for so long.¹⁸

The most likely source of these photoproducts is photolysis of sSOZ. The suggested mechanism is shown in Fig. 7. Because the O–O bonds in SOZ molecules are relatively weak, they are

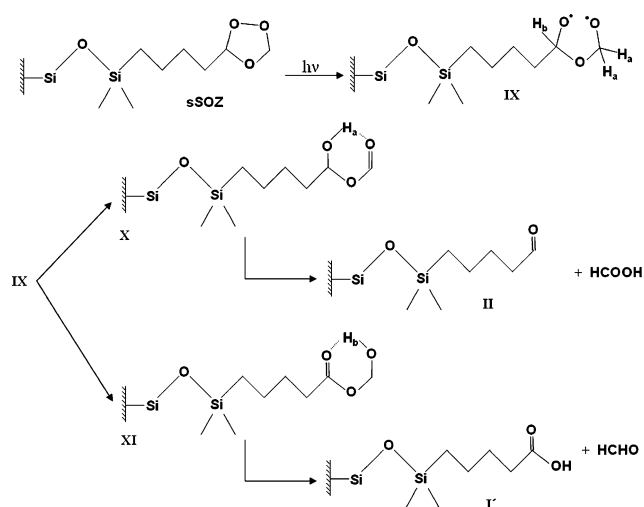


Fig. 7 Mechanism of sSOZ photolysis leading to photochemical release of HCHO and HCOOH.

easily broken by UV photons^{27–29} to produce an intermediate (IX). Rearrangement of IX can proceed *via* two possible pathways: 1,4-H_a shift and 3,5-H_b shift forming intermediate species, X and XI, respectively. Depending on the H-transfer pathway, formic acid (from X through H_a migration) or formaldehyde (from XI through H_b migration) are produced together with surface aldehyde (II) and surface acid (I').

The large delay between oxidation of the sample and photolysis experiments (several hours) implies that sSOZ in SAM do not decompose on timescales of hours at room temperature. Such high stability of substituted SOZ compounds is not unusual. For example, SOZ obtained by ozonolysis of 2,3-dimethylbutene remains stable for days in solutions³⁰ and for hours in the gas-phase at room temperature.²⁹ SOZ of many other singly-substituted molecules have been successfully prepared and characterized by analytical techniques, some of which require heating the sample (GC/MS and ESI-MS).^{21,22,29,31}

A previous study of the photolysis of 3,5-dimethyl-1,2,4-trioxolane (secondary ozonide of 2-butene)²⁹ showed that the SOZ photolytic decomposition mechanism is wavelength-dependent. The authors reported that photolysis by hard UV radiation (ArF laser, 193 nm) produced many different products, including formic acid, whereas photolysis by mild UV radiation (N₂ laser, 337 nm) was a much slower process, which could not compete with SOZ oligomerization occurring on the reactor walls under their experimental conditions. Although sSOZ oligomerization cannot be ruled out, we do not observe a change in the HCHO/HCOOH ratio over the action spectrum (Fig. 4) wavelength range of 270–310 nm.

The surface bound hydroperoxides (VI and VIII) are also expected to photolyze by cleavage of the O–OH bond releasing OH and/or H₂O and leaving surface products on the surface. The highly reactive OH radical is likely to either add to double bonds remaining on the SAM surface or abstract an H-atom from a neighboring chain. Subsequent reactions with trace O₂ molecules in the buffer gas-flow will produce surface-bound RO₂ radicals. We cannot rule out the possibility that one of

the secondary reactions involving RO₂ radicals can generate HCHO and HCOOH as secondary products of photolysis; more information on photochemistry of hydroperoxides in the condensed organic phase is necessary to address this question.

(c) Atmospheric implications

In spite of the incomplete characterization of the surface products in this work, it is clear that oxidation of unsaturated organic films by ozone has a strong effect on the photochemical properties of the resulting surface. The photodissociation cross section of the oxidized film is characteristic of absorption by peroxidic groups. This observation has important implications for photochemical aging of both primary organic aerosol (POA), which is emitted directly in particulate form, and secondary organic aerosol (SOA), formed by condensation of low volatility products of atmospheric oxidation of hydrocarbons. Indeed, a substantial fraction of POA in urban areas comes from cooking emissions^{32,33} containing an array of unsaturated organics such as oleic acid, linoleic acid, cholesterol derivatives, etc. Oxidation of these unsaturated molecules will convert them into more photoactive forms permitting further processing induced by solar radiation.

SOA formation from monoterpene oxidation by ozone has been extensively investigated,³⁴ and its aging by UV-radiation is likely to be equally important to the POA case, especially for SOA generated by ozonolysis in the dark. Several research groups are currently working in this important area.^{35,36} Presto *et al.*³⁵ reported a significant effect of UV-radiation on the yield reduction of SOA in terpene ozonolysis and concluded that SOA yield is likely to depend on actinic flux. Our preliminary measurements of the photochemical properties of SOA generated by ozonolysis of α -pinene and *d*-limonene reveal even stronger photoactivity than reported here for alkene-terminated SAM. The results on SOA photolysis will be reported elsewhere.

Photochemical processing of organic particles cannot only change their chemical properties but also serve as a potential source of free organic aldehydes and carboxylic acids. Verification of this hypothesis is an ongoing research effort in our group, and it requires a careful quantification of photodissociation cross-sections of model POA and SOA particles generated under realistic atmospheric conditions.

Conclusions

Ozonolysis of assembled organic monolayers deposited on SiO₂ nanoparticles and photolysis of the resulting oxidized surface have been studied. Such SiO₂ nanoparticles are characterized by a high surface-to-volume ratio that is ideal for investigation of surface-specific reactions occurring at the organic aerosol–air interface. The observed pattern of products implies rich chemistry resulting in the formation of complex oxygenated products on the SAM surface. Some of these products are photoactive in the tropospheric actinic window ($\lambda > 295$ nm), and release formaldehyde, formic acid, and possibly other small molecules in the gas-phase during UV irradiation. The wavelength dependence of formic acid yield strongly suggests the presence of peroxides such as secondary ozonides on the oxidized SAM surface. The main implication

of this work is the potential role of solar radiation in photoaging of primary and secondary organic aerosols.

Acknowledgements

This study was supported by the National Science Foundation through the Environmental Molecular Science Institute (EMSI) program, grant CHE-0431312, and Atmospheric Chemistry Program, grant ATM-0509248. Jiho Park was supported by the Camille and Henry Dreyfus Foundation's Postdoctoral Scholarship in Environmental Chemistry. Maggie L. Walser was supported by the National Science Foundation Graduate Research Fellowship program.

References

- 1 B. J. Finlayson-Pitts and J. N. Pitts, Jr, *Chemistry of the Upper and Lower Atmosphere: Theory Experiments, and Applications*, Academic Press, San Diego, CA, 2000.
- 2 C. A. Pope III, R. T. Burnett, M. J. Thun, E. E. Calle, D. Krewski, K. Ito and G. D. Thurston, *J. Am. Med. Assoc.*, 2002, **287**, 1132.
- 3 J. E. Penner, M. O. Andreae, H. Annegarn, L. Barrie, A. Jayaraman, R. Leaitch, D. M. Murphy, J. Nganga and G. Pitari, *Aerosols, their Direct and Indirect Effects*, Cambridge University Press, New York, 2001.
- 4 (a) G. M. Nathanson, P. Davidovits, D. R. Worsnop and C. E. Kolb, *J. Phys. Chem.*, 1996, **100**, 13007; (b) E. M. Knipping, M. J. Lakin, K. M. Foster, P. Jungwirth, D. J. Tobias, R. B. Gerber, D. Dabdub and B. J. Finlayson-Pitts, *Science*, 2000, **288**, 5464; (c) B. T. Mmerek, J. M. Hicks and D. J. Donaldson, *J. Phys. Chem. A*, 2000, **104**, 10789; (d) P. Jungwirth and D. J. Tobias, *J. Phys. Chem. A*, 2002, **106**, 379; (e) J. P. D. Abbatt, *Chem. Rev.*, 2003, **103**, 4783; (f) J. P. Reid and R. M. Sayer, *Chem. Soc. Rev.*, 2003, **32**, 70; (g) B. C. Garrett, *Science*, 2004, **303**, 1146; (h) D. F. Liu, G. Ma, L. M. Levering and H. C. Allen, *J. Phys. Chem. B*, 2004, **108**, 2252; (i) P. J. Ziemann, *Faraday Discuss.*, 2005, **130**, 469; (j) J. D. Hearn and G. D. Smith, *Phys. Chem. Chem. Phys.*, 2005, **7**, 2549; (k) R. Symes, R. M. Sayer and J. P. Reid, *Phys. Chem. Chem. Phys.*, 2004, **6**, 474.
- 5 K. Broekhuizen, P. P. Kumar and J. P. D. Abbatt, *Geophys. Res. Lett.*, 2004, **31**, L01107.
- 6 (a) R. A. Duce, V. A. Mohnen, P. R. Zimmerman, D. Grosjean, W. Cautreels, R. Chatfield, R. Jaenicke, J. A. Ogren, E. D. Pellizzari and G. T. Wallace, *Rev. Geophys.*, 1983, **21**, 921; (b) L. M. Hildemann, G. R. Markowski and G. R. Cass, *Environ. Sci. Technol.*, 1991, **25**, 744; (c) A. M. Middlebrook, D. M. Murphy and S. J. Thomson, *Geophys. Res. [Atmos.]*, 1998, **103**, 16475; (d) D. M. Murphy, J. R. Anderson, P. K. Quinn, L. M. McInnes, F. J. Brechtel, S. M. Kreidenweis, A. M. Middlebrook, M. Posfai, D. S. Thomson and P. R. Buseck, *Nature*, 1998, **392**, 62; (e) C. Alves, C. Pio and A. Duarte, *Atmos. Environ.*, 2001, **35**, 5485; (f) C. Alves, A. Carvalho and C. Pio, *J. Geophys. Res. [Atmos.]*, 2002, **107**, 8345; (g) M. Mochida, Y. Kitamori, K. Kawamura, Y. Nojiri and K. Suzuki, *J. Geophys. Res. [Atmos.]*, 2002, **107**, 4325; (h) D.-Y. Liu, R. J. Wenzel and K. A. Prather, *J. Geophys. Res. [Atmos.]*, 2003, **108**, 8426.
- 7 G. B. Ellison, A. F. Tuckand and V. Vaida, *J. Geophys. Res. [Atmos.]*, 1999, **104**, 11633.
- 8 (a) C. C. Lai, S. H. Yang and B. J. Finlayson-Pitts, *Langmuir*, 1994, **10**, 4637; (b) T. Moise and Y. Rudich, *J. Geophys. Res. [Atmos.]*, 2000, **105**, 14667; (c) T. Moise and Y. Rudich, *J. Phys. Chem. A*, 2002, **106**, 6469; (d) J. W. Morris, P. Davidovits, J. T. Jayne, J. L. Jimenez, Q. Shi, C. E. Kolb, D. R. Worsnop, W. S. Barney and G. Cass, *Geophys. Res. Lett.*, 2002, **29**, 1357; (e) V. Vaida and J. E. Headrick, *J. Phys. Chem. A*, 2000, **104**, 5401; (f) T. L. Eliason, S. Aloisio, D. J. Donaldson, D. J. Cziczo and V. Vaida, *Atmos. Environ.*, 2003, **37**, 2207.
- 9 P. S. Bailey, *Organic Chemistry, Vol 39, Part 1, Ozonation in Organic Chemistry Vol. 1 Olefinic Compounds*, Academic Press, New York, 1978.
- 10 R. Criegee, *Angew. Chem.*, 1975, **87**, 765.

- 11 (a) O. Horie and G. K. Moortgat, *Atmos. Environ., Part A*, 1991, **25A**, 1881; (b) J. H. Kroll, J. S. Clarke, N. M. Donahue, J. G. Anderson and K. L. Demerjian, *J. Phys. Chem. A*, 2001, **105**, 1554; (c) J. H. Kroll, N. M. Donahue, V. J. Cee, K. L. Demerjian and J. G. Anderson, *J. Am. Chem. Soc.*, 2002, **124**, 8518; (d) J. H. Kroll, S. R. Sahay, J. G. Anderson, K. L. Demerjian and N. M. Donahue, *J. Phys. Chem. A*, 2001, **105**, 4446; (e) S. E. Paulson, M. Y. Chung and A. S. Hasson, *J. Phys. Chem. A*, 1999, **103**, 8125; (f) A. R. Rickard, D. Johnson, C. D. McGill and G. Marston, *J. Phys. Chem. A*, 1999, **103**, 7656.
- 12 C. R. Usher, A. E. Michel, D. Stec and V. H. Grassian, *Atmos. Environ.*, 2003, **37**, 5337.
- 13 A. L. Gomez, J. Park, M. L. Walser, A. Lin and S. A. Nizkorodov, *J. Phys. Chem. A*, 2006, **110**, 3584.
- 14 Y. Dubowski, J. Vieceli, D. J. Tobias, A. L. Gomez, A. Lin, S. A. Nizkorodov, T. M. McIntire and B. J. Finlayson-Pitts, *J. Phys. Chem. A*, 2004, **108**, 10473.
- 15 Northwest-Infrared Vapor Phase Infrared Spectral Library. Pacific Northwest National Laboratory, <http://nwir.pnl.gov>.
- 16 E. R. Thomas, G. J. Frost and Y. Rudich, *J. Geophys. Res., [Atmos.]*, 2001, **106**, 3045.
- 17 C. R. Usher, A. E. Michel and V. H. Grassian, *Chem. Rev.*, 2003, **103**, 4883.
- 18 P. Neeb, F. Sauer, O. Horie and G. K. Moortgat, *Atmos. Environ.*, 1997, **31**, 1417.
- 19 R. S. Disselkamp and M. Dupuis, *J. Atmos. Chem.*, 2001, **40**, 231.
- 20 R. L. Kuczowski, *Chem. Soc. Rev.*, 1992, **21**, 79.
- 21 R. Fajgar, J. Vitek, Y. Haas and J. Pola, *Tetrahedron Lett.*, 1996, **37**, 3391.
- 22 K. Griesbaum, V. Miclaus and I. C. Jung, *Environ. Sci. Technol.*, 1998, **32**, 647.
- 23 R. Fajgar, J. Vitek, Y. Haas and J. Pola, *J. Chem. Soc., Perkin Trans. 2*, 1999, **239**.
- 24 M. A. Dreyfus, M. P. Tolocka, S. M. Dodds, J. Dykins and M. V. Johnston, *J. Phys. Chem. A*, 2005, **109**, 6248.
- 25 H.-M. Hung, Y. Katrib and S. T. Martin, *J. Phys. Chem. A*, 2005, **109**, 4517.
- 26 T. M. McIntire, A. S. Lea, D. J. Gasper, N. Jaitly, Y. Dubowski, Q. Q. Li and B. J. Finlayson-Pitts, *Phys. Chem. Chem. Phys.*, 2005, **7**, 3605.
- 27 M. Hawkins, C. K. Kohlmler and L. Andrews, *J. Phys. Chem.*, 1982, **86**, 3154.
- 28 L. Andrews and C. K. Kohlmler, *J. Phys. Chem.*, 1982, **86**, 4548.
- 29 L. Khachatryan, Y. Haas and J. Pola, *J. Chem. Soc., Perkin Trans. 2*, 1997, 1147.
- 30 K. Griesbaum, W. Volpp, R. Greinert, H. J. Greunig, J. Schmid and H. Henke, *J. Org. Chem.*, 1989, **54**, 383.
- 31 (a) K. Griesbaum, W. Volpp, R. Greinert, H. J. Greunig, J. Schmid and H. Henke, *J. Org. Chem.*, 1989, **54**, 383; (b) K. Griesbaum, M. Hils and J. Bosch, *Tetrahedron*, 1996, **52**, 14813.
- 32 L. M. Hildemann, M. A. Mazurek, G. R. Cass and B. R. T. Simoneit, *Environ. Sci. Technol.*, 1991, **25**, 1311.
- 33 J. J. Schauer, M. J. Kleeman, G. R. Cass and B. R. T. Simoneit, *Environ. Sci. Technol.*, 1999, **33**, 1566.
- 34 (a) T. Hoffmann, J. Odum, F. Bowman, D. Collins, D. Kluckow, R. Flagan and J. H. Seinfeld, *J. Atmos. Chem.*, 1997, **26**, 189; (b) M. Jang, R. Kamens, K. Leach and M. Strommen, *Environ. Sci. Technol.*, 1997, **31**, 2805; (c) R. Griffin, D. Cocker, R. Flagan and J. Seinfeld, *J. Geophys. Res., [Atmos.]*, 1999, **104**, 3555; (d) Y. Iinuma, O. Bogo, T. Gnauk and H. Hermann, *Atmos. Environ.*, 2004, **38**, 761.
- 35 A. A. Presto, K. E. H. Hartz and N. M. Donahue, *Environ. Sci. Technol.*, 2005, **39**, 7036.
- 36 J. D. Surratt, S. M. Murphy, J. H. Kroll, N. L. Ng, L. Hildebrandt, A. Sorooshian, R. Szmigielski, R. Vermeylen, W. Maenhaut, M. Claeys, R. C. Flagan and J. H. Seinfeld, *J. Phys. Chem. A* submitted.